ChemPubSoc Europe

DOI: 10.1002/ejic.201600084

EurJIC European Journal of Inorganic Chemistry

Full Paper

Water-Soluble Complexes

Neutral 1,3,5-Triaza-7-phosphaadamantane-Ruthenium(II) Complexes as Precursors for the Preparation of Highly Water-Soluble Derivatives

Federica Battistin,[a] Gabriele Balducci,[a] Elisabetta Iengo,[a] Nicola Demitri,[b] and Enzo Alessio*[a]

Abstract: The monodentate phosphane ligand 1,3,5-triaza-7-phosphaadamantane (PTA) imparts excellent water solubility to its complexes. We aimed to prepare precursors with one or more PTA coligands for solubility and one or more labile ligands for facile replacement by a linker. For this purpose, we investigated the reactivity of the neutral isomers *trans*- and *cis*-$RuCl_2(PTA)_4$ (**1** and **2**) towards 2,2′-bipyridine (bpy), as a model chelating diimine linker. The new derivatives *mer*-[Ru(bpy)Cl(PTA)$_3$]Cl (**9**) and *fac*-[Ru(bpy)Cl(PTA)$_3$]Cl (**10**) were prepared and characterized. We also found that PTA reacts rapidly with *cis*,*fac*-$RuCl_2$(dmso-*O*)(dmso-*S*)$_3$ (**11**) and *trans*-$RuCl_2$(dmso-*S*)$_4$ (**13**) under mild conditions through the replacement of pairs of mutually *trans* dmso ligands with high selectivity, even when in stoichiometric defect. Thus, **11** affords *cis*,*cis*,*trans*-$RuCl_2$(dmso-*S*)$_2$(PTA)$_2$ (**12**), whereas **13** gives **1**. The two dmso ligands of **12** can be replaced selectively by chelating diimines such as bpy to afford the less symmetrical all-*cis* product *cis*,*cis*-Ru(bpy)Cl_2(PTA)$_2$ (**16**).

1. Introduction

The cagelike monodentate phosphane 1,3,5-triaza-7-phosphaadamantane (PTA), first reported in 1974 by Daigle and co-workers,[1] is an amphiphilic, air-stable, neutral ligand, which is soluble in several organic solvents and characterized by a high solubility in water (ca. 235 g/L) by virtue of H bonding to the tertiary amine nitrogen atoms. At moderately acidic pH (pK_a = 5.89),[2] the regioselective protonation of one N atom generates $PTAH^+$. The coordination chemistry of PTA has been reviewed thoroughly by Peruzzini and co-workers.[3] It typically binds strongly to metal ions through the P atom in a monodentate fashion. It has moderate steric demand (cone angle 103°), good σ- and π-bonding abilities [comparable to those of $P(OMe)_3$] and, above all, it typically imparts excellent water solubility to its complexes. By virtue of their solubility, PTA–metal complexes have been investigated as homogeneous catalysts, either directly in aqueous solution or under aqueous–organic biphasic conditions,[3–11] and as potential anticancer drugs.[8,12–17] Among these drug candidates, the most well-known are the organometallic RAPTA-type compounds [$RuCl_2(\eta^6$-arene)(PTA)] (RAPTA = ruthenium–arene PTA) developed by the group of Dyson.[12]

We are particularly interested in the design and synthesis of suitable Ru^{II} precursors for the preparation of water-soluble ruthenium–porphyrin conjugates for investigation in the fields of supramolecular chemistry[18] and photodynamic therapy.[19] In this context, the leaving ligands in the ideal metal precursor need to match, in terms of number and geometry, the binding preferences of the bifunctional linker used to connect the porphyrin(s). Typically, in our case, the linker can be either a monodentate pyridyl ring (such as in *meso*-pyridylporphyrins),[18] a chelating diimine such as 4′-methyl-2,2′-bipyridine-4-carboxylic acid (bpyAc, Figure 1)[19,20] or 2-(2′-pyridyl)pyrimidine-4-carboxylic acid (cppH, Figure 1),[21,22] or a tridentate facial ligand such as a functionalized 1,4,7-triazacyclononane (TACN).[23]

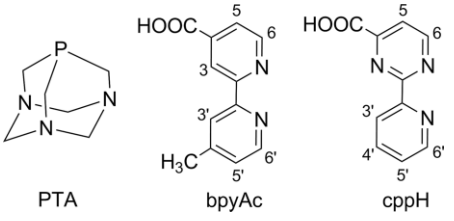

Figure 1. PTA (left) and the diimine linkers bpyAc (center) and cppH (right) with proton numbering scheme.

Previously, we have largely exploited Ru^{II}–dmso (dmso = dimethyl sulfoxide)[18,22,24] and Ru^{II}–[9]aneS3 precursors ([9]aneS3 = 1,4,7-trithiacyclononane).[19,21,25] Nevertheless, al-

[a] *Department of Chemical and Pharmaceutical Sciences, University of Trieste,*
Via L. Giorgieri 1, 34127 Trieste, Italy
E-mail: alessi@units.it
http://dscf.units.it/en/department/people/alessio-enzo/1055
[b] *Elettra - Synchrotron Light Source,*
S.S. 14 Km 163.5, Area Science Park, 34149 Basovizza, Trieste, Italy
Supporting information and ORCID(s) from the author(s) for this article are available on the WWW under http://dx.doi.org/10.1002/ejic.201600084.

though most of them are well-behaved in terms of reactivity, they did not provide sufficient solubility in water, which is a highly desirable feature both in the design of efficient host molecules in supramolecular chemistry and in medicinal inorganic chemistry. For this reason, we decided to investigate if the neutral complexes *trans*- and *cis*-$RuCl_2(PTA)_4$ (**1** and **2**, respectively) could be exploited as precursors for the preparation of water-soluble conjugates. Even though these isomers and the neglected Ru^{III} complex *trans*-$[RuCl_4(PTAH)_2]Cl$ (**3**) have been known for many years[3,5,26,27] and have been used as catalysts in several reactions (very often the isomer employed was not specified),[3–7] their reactivity is largely unexplored. In this manuscript, we report a thorough investigation of the chemical behavior of the isomers **1** and **2** in water and other coordinating solvents as well as their reactivity towards 2,2′-bipyridine (bpy), which was used as a model for chelating diimine linkers (i.e., cppH and bpyAc). Such linkers might allow us to connect a $\{RuCl_x(PTA)_y\}$ fragment ($x = 0–2$, $y = 2–4$, $x + y = 4$) to an appropriately functionalized porphyrin through the formation of an amidic or esteric bond.[19,20] The new derivatives *mer*-$[Ru(bpy)Cl(PTA)_3]Cl$ (**9**) and *fac*-$[Ru(bpy)Cl(PTA)_3]Cl$ (**10**) were prepared and characterized.

In addition, we also investigated the reactivity of the well-known $Ru^{II}Cl$(dmso) complexes *cis*,*fac*-$RuCl_2$(dmso-*O*)(dmso-*S*)$_3$ (**11**) and *trans*-$RuCl_2$(dmso-*S*)$_4$ (**13**) towards PTA. An ideal precursor might have one or more PTA coligands for solubility and one or more dmso ligands (with appropriate geometry) for facile replacement by the linker. We confirmed and expanded the results originally reported by Kathó and co-workers on this topic[11] and investigated the unexplored reactivity of the Ru^{II} complex *cis*,*cis*,*trans*-$RuCl_2$(dmso-*S*)$_2(PTA)_2$ (**12**) towards bpy and bpyAc and obtained *cis*,*cis*-$Ru(bpy)Cl_2(PTA)_2$ (**16**) and *cis*,*cis*-$Ru(bpyAc)Cl_2(PTA)_2$ (**17**, as a 50:50 mixture of the two stereoisomers **17a** and **17b**).

2. Results and Discussion

2.1. *trans*-$RuCl_2(PTA)_4$ (1) and *cis*-$RuCl_2(PTA)_4$ (2)

The controversial story of the preparation and characterization of the neutral isomers *trans*- and *cis*-$RuCl_2(PTA)_4$, which started in 1992 with the report of Darensbourg and co-workers[5] and was eventually concluded by Mebi and Frost 15 years later,[26] has already been reviewed.[3] In short, **1** is the kinetic product of the synthetic procedure from hydrated $RuCl_3$ and it isomerizes to the thermodynamically stable *cis* isomer **2** in aqueous solution. Later, Romerosa and co-workers established that light can play an important role in the interconversion of the two isomers.[27]

We prepared compound **1** as described in the literature (Scheme 1).[5]

In an unsuccessful attempt to prepare the presumed Ru^{III} and Ru^{II} intermediates *trans*-$[RuCl_4(PTAH)_2]Cl$ (**3**) and *trans*-$RuCl_4(PTAH)_2$ (**4**), respectively, which had been occasionally isolated in the recrystallization of **1**,[5,28] we found that the reaction between hydrated $RuCl_3$ and PTA in ethanol also occurs at room temperature, even though it is very slow (days) and affords low yields of **1**. The Ru^{III} compound **3** was instead prepared selectively in high yield by a different route, that is, by the treatment of the Ru^{III}–dmso precursor $[(dmso)_2H]$*trans*-$[RuCl_4$(dmso-*S*)$_2]$ with PTA in MeOH/HCl mixtures.[29]

In our hands, the best synthetic procedure for the preparation of **2** was the irradiation of an aqueous solution of **1** with blue light (λ = 470 nm) for 1 h.[27] The evaporation of the solvent afforded pure **2** quantitatively (according to NMR spectroscopy analysis). The isomerization of **1** could also be performed thermally by heating an aqueous solution to reflux (1 h). However, the ^{31}P NMR spectrum suggested that the thermal reaction was not as clean as the photochemical one and led to the formation of byproducts, including PTA oxide (PTAO),[1] characterized by a sharp singlet at δ = –2.1 ppm in the ^{31}P NMR spectrum. With hydrated $RuBr_3$ as a precursor and the same synthetic procedures described above, we isolated the corresponding and unprecedented bromo complexes *trans*-$RuBr_2(PTA)_4$ and *cis*-$RuBr_2(PTA)_4$ in good yields and characterized them.[29]

A complete NMR spectroscopy characterization of **1** and **2** is reported in Table 1. The ^1H and ^{31}P NMR spectra of **1** in $CDCl_3$ are quite straightforward, owing to the high symmetry of the complex. The ^{31}P NMR spectrum of **2**, consistent with the A_2X_2 spin system, presents two equally intense triplets at δ = –24.1 and –59.4 ppm ($^2J_{P,P}$ = 28.6 Hz). On the basis of the spectrum of **1** (Table 1) and literature data,[3] the most shielded triplet was assigned to the pair of mutually *trans* PTA ligands. The previously unreported ^1H NMR spectrum of **2** in $CDCl_3$ (contrary to previous reports, **2** is considerably less soluble than **1** in this solvent)[27] is more complex and consists of two relatively broad singlets (12 H each) at δ = 4.04 and 4.47 ppm and a multiplet (24 H) centered at δ = 4.48 ppm (Supporting Information, Figure S4). The singlets (or better, unresolved multiplets) belong to the NCH_2P groups of the two pairs of equivalent PTA ligands: in the H–H COSY spectrum, they are both coupled to the multiplet (generated by the NCH_2N groups), whereas in the heteronuclear single quantum coherence (HSQC) spectrum (Figure S5) they have distinct cross-peaks with carbon atoms that resonate in the NCH_2P region (Table 1). Thus, the ^1H and ^{13}C resonances of the NCH_2P groups are sensitive to the PTA position in the complex. A ^1H–^{31}P HMBC spectrum (Figure S6) allowed us to

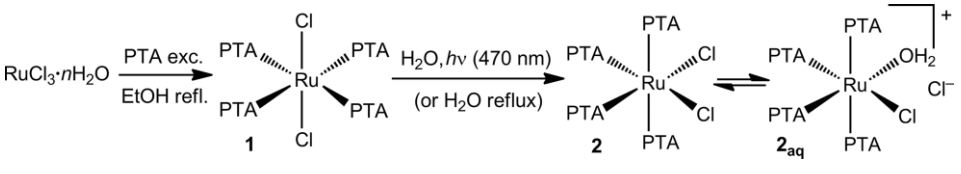

Scheme 1. Preparation of isomers **1** and **2**.

Table 1. ^{1}H, ^{13}C, and ^{31}P NMR chemical shifts δ [ppm] and coupling constants J [Hz] of **1**, **2**, and $\mathbf{2}_{aq}$.

	^{1}H (J)	$^{13}C\{^{1}H\}$	$^{31}P\{^{1}H\}$ (J)	Solvent
trans-$RuCl_2(PTA)_4$ (**1**)	4.61, 4.57 (13.7), AB q, 24 H, NCH_2N	73.3, NCH_2N	–50.6, s, mutually *trans* PTAs	$CDCl_3$
	4.40, br. s, 24 H, NCH_2P	53.1, NCH_2P		
cis-$RuCl_2(PTA)_4$ (**2**)	4.48, m, 24 H, NCH_2N	73.1, NCH_2N		$CDCl_3$
	4.47, br. s, 12 H, NCH_2P, mutually *trans* PTAs	54.0, NCH_2P	–59.4 (28.6), t, mutually *trans* PTAs	
	4.04, br. s, 12 H, NCH_2P, PTA *trans* to Cl	58.7, NCH_2P	–24.1 (28.6), t, PTA *trans* to Cl	
trans-$RuCl_2(PTA)_4$ (**1**)	4.63, br. s, 24 H, NCH_2N	70.8, NCH_2N	–49.6, s, mutually *trans* PTAs	D_2O
	4.35, br. s, 24 H, NCH_2P	50.8, NCH_2P		
cis-$RuCl_2(PTA)_4$ (**2**)	4.65, m, 24 H, NCH_2N	n.d.	–21.6 (28.5), t, PTA *trans* to Cl	D_2O[a]
	4.47, br. s, 12 H, NCH_2P, mutually *trans* PTAs		–57.6 (28.5), t, mutually *trans* PTAs	
cis-$[RuCl(OH_2)(PTA)_4]^+$ ($\mathbf{2}_{aq}$)	4.59, m, 24 H, NCH_2N	70.3, NCH_2N	–12.7 (30.3, 34.8), dt, PTA *trans* to OH_2	D_2O
	4.26, d, 12 H, NCH_2P	49.8, NCH_2P	–22.7 (26.1, 34.8), dt, PTA *trans* to Cl	
	4.11, s, 6 H, NCH_2P	54.9, NCH_2P	–52.6 (26.1, 30.3), dd, mutually *trans* PTAs	
	3.97, s, 6 H NCH_2P	54.6, NCH_2P		

[a] Recorded in the presence of ca. 1 M NaCl.

assign unambiguously the two NCH_2P singlets in the ^{1}H NMR spectrum, which are pairwise related to the two triplets in the ^{31}P dimension. The shielded singlet, which has a cross-peak with the ^{31}P triplet at δ = –24.1 ppm, was assigned to the PTA ligands *trans* to Cl ligands, and the other was assigned to the mutually *trans* PTA ligands.

We also reinvestigated the behavior of the two isomers in aqueous solution. In agreement with published data,[27] **2** equilibrates rapidly with the monoaqua species *cis*-$[RuCl(OH_2)(PTA)_4]^+$ ($\mathbf{2}_{aq}$), which was isolated as a PF_6^- salt by following another synthetic route (see below). The ^{31}P NMR resonances of the mixture of **2** and $\mathbf{2}_{aq}$ were readily distinguished in a P–P COSY spectrum (Figure S7). The integration of such resonances afforded an equilibrium constant $K = 1.39 \times 10^{-2}$ M. The ^{31}P NMR spectrum of $\mathbf{2}_{aq}$ presents an AM_2X spin system (Table 1) with multiplets centered at δ = –12.7 (PTA *trans* to OH_2), –22.7 (PTA *trans* to Cl), and –52.6 ppm (mutually *trans* PTA ligands). The assignments are consistent with the multiplicity and intensity of each signal, as well as with the spectrum of **2** and literature data.[27] The ^{1}H NMR spectrum of the mixture **2** and $\mathbf{2}_{aq}$ is quite complex. According to the ^{31}P NMR spectrum, pure **2** was obtained upon the addition of an excess of NaCl (ca. 1 M) to the D_2O solution. The previously unreported ^{1}H NMR spectrum of **2** in D_2O (Table 1) is quite similar to that recorded in $CDCl_3$. The release of the second chlorido ligand from $\mathbf{2}_{aq}$ and the formation of the diaqua species *cis*-$[Ru(OH_2)_2(PTA)_4]^{2+}$ (**5**), which is characterized by two equally intense triplets in the ^{31}P NMR spectrum at δ = –16.0 ($^{2}J_{P,P}$ = 27.1 Hz, PTA *trans* to OH_2) and –45.9 ppm (mutually *trans* PTA ligands), became apparent for concentrations of **2** below 5 mM. This species was obtained previously upon the addition of an excess of PTA to a solution of $[Ru(OH_2)_6]^{2+}$.[2] The treatment of an aqueous solution of **2** with 1 equiv. of $AgCF_3SO_3$ for 48 h at room temperature afforded the triflate salt of $\mathbf{2}_{aq}$, *cis*-$[RuCl(OH_2)(PTA)_4][CF_3SO_3]$, in moderate yield.[27] The chloride abstraction was accompanied by the formation of Ag, Ag_2O (the AgCl precipitate was dark grey), or both. Attempts to remove the second chlorido ligand from **2** by increasing the Ag^+/Ru ratio and to isolate the corresponding dicationic salt *cis*-$[Ru(OH_2)_2(PTA)_4][CF_3SO_3]_2$ were unsuccessful.

Contrary to previous reports,[27] we found that a light-protected D_2O solution of **1** is perfectly stable at room temperature: the NMR spectra remained unchanged for days (Figure S3). On the contrary, the exposure of the NMR tube to diffuse indoor light induced the slow isomerization (days) of **1** to a mixture of **2** and $\mathbf{2}_{aq}$, as shown by the appearance of the corresponding resonances in the ^{31}P NMR spectrum.

We also investigated the thermal stability of **1** in the coordinating solvents DMSO and CH_3CN. When a concentrated solution of **1** in DMSO (in which the complex is only partially soluble) was heated to 150 °C for 4 h, complete thermal isomerization to the *cis* isomer **2** (which partially precipitates from the warm solution) was observed. When the reaction was performed at lower temperatures, a pale yellow solid was isolated upon the addition of acetone. On the basis of the ^{31}P NMR spectrum, this precipitate is a mixture of **2** and an intermediate characterized by an AX_2 spin system: a triplet at δ = –25.6 ppm is attributable to a PTA ligand *trans* to Cl, and a doublet at δ = –61.0 ppm ($^{2}J_{P,P}$ = 27.9 Hz) is in the region for mutually *trans* PTA ligands (Figure S8). In addition to several PTA peaks, the ^{1}H NMR spectrum shows a singlet at δ = 3.20 ppm, which is attributable to a dmso-*S* ligand in a symmetrical environment (equivalent methyl groups). On the basis of this spectral evidence, the intermediate species was identified as *cis*,*mer*-$RuCl_2(dmso\text{-}S)(PTA)_3$ (**6**, Figure 2). The intermediate **6** could not be isolated in pure form: the highest **6**/**2** ratio (40:60, without residual **1**) was obtained by performing the reaction at 70 °C for 1 h.

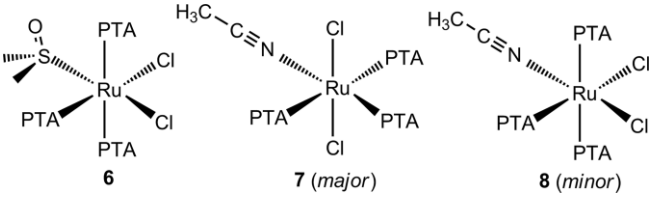

Figure 2. Intermediates isolated (not in pure form) when the thermal isomerization of **1** to **2** was performed in DMSO (**6**) or acetonitrile (**7** and **8**).

A similar behavior was observed when **1** was heated in acetonitrile. In this case, the complex dissolves completely under reflux conditions and a pale yellow solid precipitates spontaneously from the solution. On the basis of the ^{31}P NMR spectrum (Figures S9–S10), the solid is a mixture of **2** (the amount of which increases with the reflux time) and the two intermedi-

ates **7** (major) and **8** (minor), both of which are characterized by AX_2 spin systems (Figure 2). On the basis of the chemical shifts of the multiplets, the major intermediate **7** (triplet at δ = –16.1 ppm, doublet at δ = –53.3 ppm, $^2J_{P,P}$ = 28.5 Hz) was identified as *trans*,*mer*-$RuCl_2(CH_3CN)(PTA)_3$, whereas the minor one (triplet at δ = –24.0 ppm, doublet at δ = –54.3 ppm, $^2J_{P,P}$ = 37.2 Hz) was identified as *cis*,*mer*-$RuCl_2(CH_3CN)(PTA)_3$ (i.e., **8** is the counterpart of **6** isolated in DMSO). In addition to the overlapped PTA resonances, the corresponding ^{1}H NMR spectrum consistently shows two singlets at δ = 2.30 and 2.46 ppm in the same ratio as the resonances of **7** and **8** in the ^{31}P NMR spectrum, and these resonances are attributed to coordinated CH_3CN.

2.2. Reactivity of 1 and 2 towards bpy

Even though PTA binds strongly to Ru^{II} centers, the above-reported results suggest that the replacement of at least one chlorido ligand and one PTA ligand from isomers **1** and **2** seems to be possible, depending on the solvent and reaction conditions. Thus, we investigated the reactivity of **1** and **2** towards bpy as a model for the diimine linkers bpyAc and cppH (Figure 1).

Both **1** and **2** reacted with bpy in water under reflux (under light-free conditions), as evidenced by a progressive color change of the solution from pale to deep yellow. More specifically, the treatment of **1** with 1 equiv. of bpy in water under reflux (1 h), followed by the evaporation of the solvent, afforded almost quantitatively the complex *mer*-[Ru(bpy)Cl(PTA)$_3$]Cl (**9**, Scheme 2).

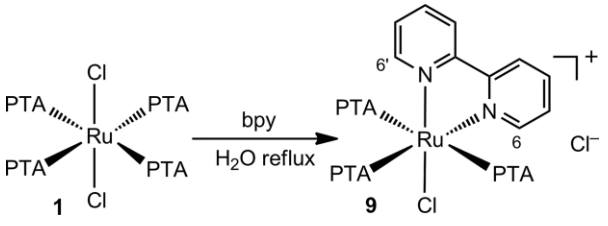

Scheme 2. Preparation of *mer*-[Ru(bpy)Cl(PTA)$_3$]Cl (**9**) upon the treatment of **1** with bpy in water under reflux.

Compound **9** was characterized by NMR spectroscopy and mass spectrometry (as a PF_6 salt, see the Experimental Section), and its single-crystal X-ray structure was also determined (Figure 3). The ^{1}H NMR spectrum (Figures S11–S14) shows eight aromatic resonances, typical of bpy in an unsymmetrical environment. In agreement with previous findings,[21,22] the most deshielded doublet was assigned to 6-H, that is, the proton with a partial positive charge that points towards the adjacent chlorido ligand (Scheme 2). The PTA region of the spectrum consists of two similar and partially overlapping sets of equally intense signals, an AB quartet and a broad singlet, in a 1:2 ratio. The most intense and upfield-shifted set was attributed to the two equivalent *trans* PTA ligands, the protons of which fall in the shielding cone of the adjacent bpy ligand. The HSQC spectrum established that the deshielded quartet in each set belongs to the NCH_2N protons and that the singlet belongs to the NCH_2P protons. The ^{31}P NMR spectrum (Figure S15) consists of an AX_2 spin system: a triplet at δ = –30.2 ppm attributable to a PTA *trans* to N, and doublet at δ = –47.6 ppm ($^2J_{P,P}$ = 32.8 Hz) for the mutually *trans* PTA ligands. The spectra did not change upon the addition of NaCl; therefore, they can be safely attributed to the intact *mer*-[Ru(bpy)Cl(PTA)$_3$]$^+$ cation (see below). Interestingly, the crystals of **9** obtained upon the recrystallization of the raw product from water/ethanol contain a network of water molecules distributed in parallel rows along the [001] direction, and these water molecules arguably contribute to the cohesive energy of the crystal through hydrogen bonding to the N atoms of the PTA moieties. The coordination distances are in general agreement with the known *trans* influence of the ligands: thus, the Ru–P bonds of the two *trans* PTA ligands [2.3427(5) and 2.3275(5) Å] are slightly longer than the Ru–P bonds *trans* to N [2.3018(5) Å], and the Ru–N bond *trans* to P [2.1154(14) Å] is longer than that *trans* to Cl [2.0770(13) Å].

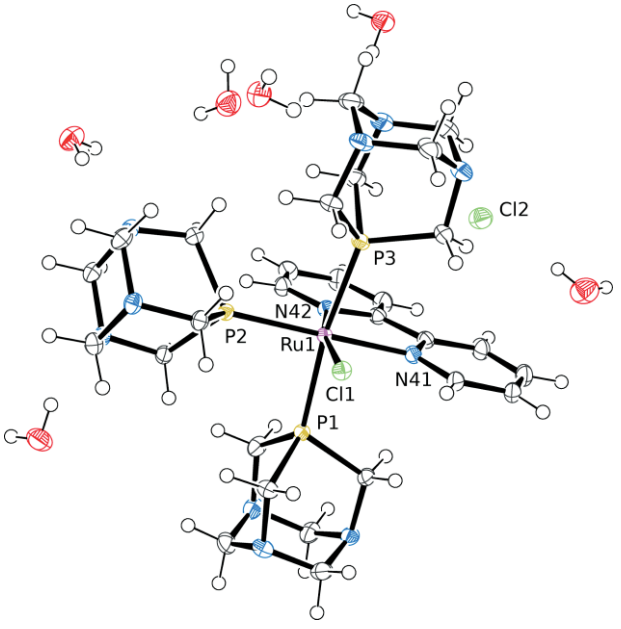

Figure 3. Molecular structure (50 % probability ellipsoids) of *mer*-[Ru(bpy)Cl(PTA)$_3$]Cl·6H_2O (**9**).

The reaction between **2** and bpy is slower and less selective: when a slight excess of bpy was used (bpy/Ru = 1.5), full conversion required ca. 10 h of reflux. According to the NMR spectra, the final mixture contained compound **9** as the main product and another species identified as *fac*-[Ru(bpy)Cl(PTA)$_3$]Cl (**10**; **9**/**10** ≈ 10) in addition to some unidentified minor species and PTAO. We found that an increase of the bpy/Ru ratio from 1.5 to 5, together with the addition of 1 equiv. of $AgNO_3$, led to the full conversion of **2** after 1 h of reflux. In addition, the main product in this case was the *fac* isomer **10** (**10**/**9** ≈ 7, Scheme 3), which was obtained in pure form for unambiguous characterization as the PF_6 salt (**10**PF_6, see Experimental Section). An increase of the reaction time involved a progressive decrease of the **10**/**9** ratio, which suggests that **10** is the kinetic product of the reaction between **2** and bpy, whereas **9** is thermodynamically more stable.

Immediately after the dissolution of **10** in D_2O, the ^{1}H NMR spectrum has only four aromatic resonances, in accord with a

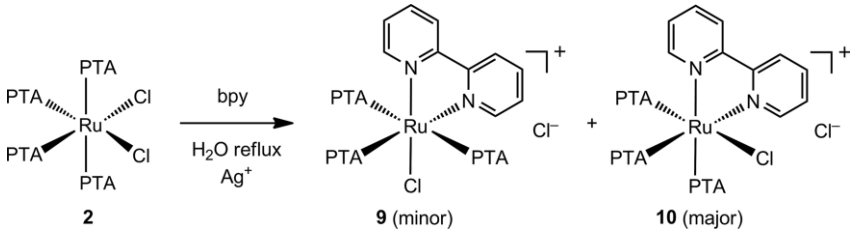

Scheme 3. Preparation of a mixture of the cationic isomers *mer*-[Ru(bpy)Cl(PTA)$_3$]Cl (**9**) and *fac*-[Ru(bpy)Cl(PTA)$_3$]Cl (**10**) upon the reaction of **2** with bpy in water under reflux.

symmetrical coordination for bpy. However, a second set of four bpy resonances, each one shifted slightly downfield with respect to the parent one and attributed to the aqua species *fac*-[Ru(bpy)(OH$_2$)(PTA)$_3$]$^{2+}$ (**10**$_{aq}$), grows slowly with time at the expense of the original one (Figure S16). Equilibrium (**10**/**10**$_{aq}$ = ca. 1.5) was reached within 24 h at room temperature. Consistently, the ^{31}P NMR spectrum shows two AX$_2$ spin systems, attributed (on the basis of their relative intensities and time evolution) to **10** (triplet at δ = –24.3 ppm, PTA *trans* to Cl) and **10**$_{aq}$ (triplet at δ = –17.7 ppm, PTA *trans* to OH$_2$; Figures S17 and S18). The two doublets overlap almost completely at δ = –44.2 ppm, that is, in the typical region for a PTA ligand *trans* to a N atom ($^2J_{P,P}$ = 29.2 Hz). The PTA region of the ^{1}H NMR spectrum is quite complicated owing to the overlapping resonances of **10** and **10**$_{aq}$. It simplifies upon the addition of an excess of NaCl (ca. 1 M), which reverts the equilibrium completely towards **10**. Under these conditions, the spectrum is similar to that of **9**, but it is the less intense set of signals, attributed to the PTA ligand *trans* to Cl, that is shielded by bpy in this case. Taken together, the NMR features are totally consistent with the proposed geometry. The single-crystal X-ray diffraction data of crystals of the protonated derivative *fac*-[Ru(bpy)Cl(PTAH)$_{2.5}$(PTA)$_{0.5}$][ClO$_4$]$_{3.5}$•2.5H$_2$O, which was obtained upon the addition of HClO$_4$ to an aqueous solution of **10**, allowed us to confirm the geometry of the complex (Figure S41).

In conclusion, we found that the coordination of bpy to **1** and **2** in aqueous solution involves the replacement of one chlorido ligand and one PTA ligand to afford the two isomers **9** and **10**, depending on the conditions. Notably, the formation of **10** was not observed in the reaction between **1** and bpy; therefore, the mechanisms of the two substitution reactions are different.

Consistent with these findings, the reactivity of both isomers **1** and **2** with bpy in organic solvents in which chloride release is unfavorable (e.g., CH$_3$CN and CHCl$_3$) is much less pronounced or altogether negligible. For example, no reaction was observed between **2** and bpy in chloroform under reflux, whereas **1** reacted to a minor extent to afford (after 5 h) a complex mixture of products that contained **2**, **10**, PTAO, and other minor uncharacterized species on the basis of the ^{31}P NMR spectrum.

2.3. Reactions of Ru^{II}–dmso Complexes with PTA

After we started our work, we became aware that the reactivity of *cis*,*fac*-RuCl$_2$(dmso-*O*)(dmso-*S*)$_3$ (**11**) towards PTA had been investigated recently by Kathó and co-workers.[11] In good agreement with their results, we found that the treatment of **11** with PTA at room temperature leads selectively to the formation of *cis*,*cis*,*trans*-RuCl$_2$(dmso-*S*)$_2$(PTA)$_2$ (**12**), regardless of the nature of the solvent (e.g., in MeOH) or the PTA/Ru ratio (Scheme 4). Even with less than 2 equiv. of PTA, compound **12** was obtained together with unreacted precursor. The replacement of all dmso-*S* ligands (with the formation of a mixture of **1**, **2**, and **12**) was observed when the reaction (PTA/Ru = 4) was performed in MeOH under reflux. Conversely, we found that the treatment of *trans*-RuCl$_2$(dmso-*S*)$_4$ (**13**, not investigated before) with PTA at room temperature leads exclusively to **1** (Scheme 4). In this case, the nature of the product does not depend on the PTA/Ru ratio employed. For example, when PTA/Ru = 2, an approximately 1:1 mixture of **1** and unreacted precursor was recovered. No intermediate could be detected; this suggests that the replacement of two *trans* dmso ligands by two PTA ligands occurs rapidly and quantitatively. As already mentioned (see above), the same behavior, that is, facile substitution of two *trans* dmso-*S* ligands, was also observed with [(dmso)$_2$H]*trans*-[RuCl$_4$(dmso-*S*)$_2$] to afford **3**.[29]

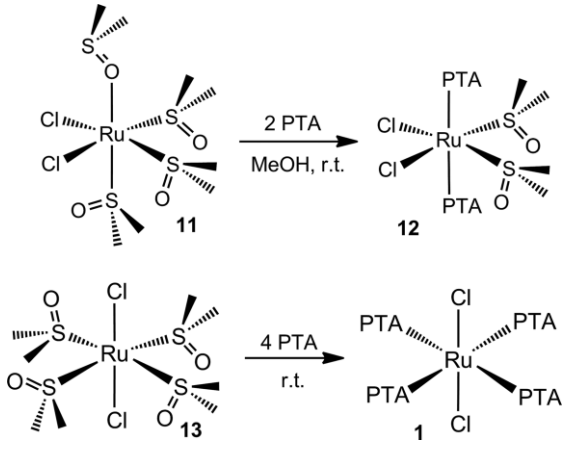

Scheme 4. Reactivity of *cis*,*fac*-RuCl$_2$(dmso-*O*)(dmso-*S*)$_3$ (**11**, top) and *trans*-RuCl$_2$(dmso-*S*)$_4$ (**13**, bottom) towards PTA at room temperature.

The spectroscopic characterization of **12** (Figure S21) as well as its X-ray structure (Figure 4) are in good agreement with previous reports.[11,30]

Compound **12** is highly soluble in water, DMSO, CHCl$_3$, and CH$_2$Cl$_2$ and also soluble in warm MeOH and EtOH. We observed that the ^{1}H NMR spectrum of a light-protected D$_2$O solution of **12** changes very slowly (days) at room temperature (Figure S20). As no signals for free DMSO or PTA were detected, the

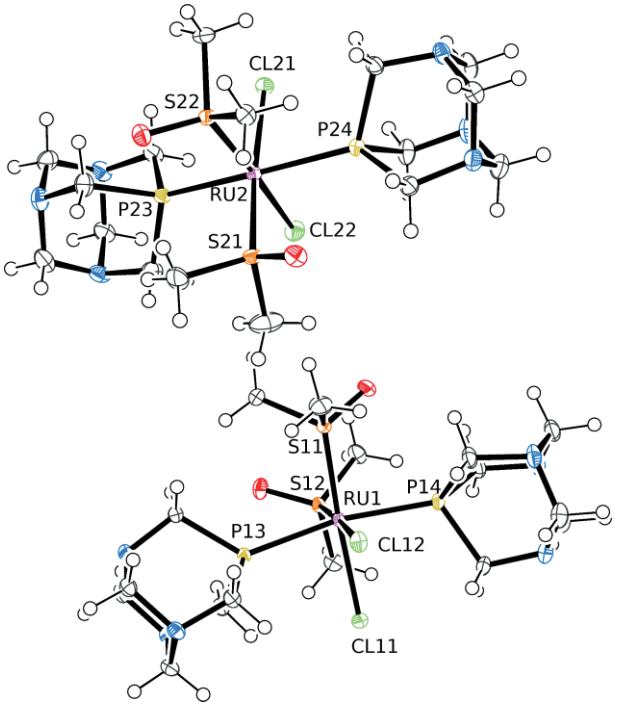

Figure 4. Molecular structure (50 % probability ellipsoids) of the two crystallographically independent units of *cis*,*cis*,*trans*-$RuCl_2(dmso\text{-}S)_2(PTA)_2$ (**12**). Disordered and underoccupied methanol and water crystallization molecules have been omitted for clarity.

spectral changes were attributed to the progressive release of a chlorido ligand to form the monoaqua species *cis*,*cis*,*trans*-$[RuCl(OH_2)(dmso\text{-}S)_2(PTA)_2]^+$ (**12**$_{aq}$). Consistent with this hypothesis, a new singlet at δ = –53.0 ppm in the ^{31}P NMR spectrum grows slowly at the expense of the original one at δ = –57.9 ppm (Figure S21). In the ^1H NMR spectrum, in addition to new signals in the PTA region, two new singlets for dmso-*S* grow at δ = 3.37 and 3.41 ppm (i.e., very close to the original singlet at δ = 3.38 ppm). In **12**$_{aq}$, although the two *trans* PTA ligands are still equivalent, the two dimethyl sulfoxide ligands are not.

We also investigated the possibility of obtaining complexes with either five or six bound PTA moieties by using the cationic Ru^{II}–dmso precursors *cis*,*fac*-$[RuCl(dmso\text{-}O)_2(dmso\text{-}S)_3][PF_6]$ (**14**) and *fac*-$[Ru(dmso\text{-}O)_3(dmso\text{-}S)_3][CF_3SO_3]_2$ (**15**), respectively. We found that the treatment of **14** with 5 equiv. of PTA in methanol at room temperature afforded *cis*-$[RuCl(OH_2)(PTA)_4][PF_6]$ (**2**$_{aq}$) in moderate yield. The ^1H NMR spectrum of the complex in D_2O corresponds to that of **2**$_{aq}$ observed in equilibrium with **2** (see above) with an additional singlet for free MeOH (crystallization molecule). The nature of the compound was also confirmed by a low-quality X-ray structural determination (Figure S42). Repeated attempts to obtain better crystals were unsuccessful. When the same reaction was performed at reflux temperature, the precipitation of **2** occurred, and the resonances of **2**$_{aq}$, **5**, and PTAO were found in the ^{31}P NMR spectrum of the mother liquor (D_2O). As there is no external chloride source, this finding suggests that the disproportionation of **2**$_{aq}$ into dichlorido (**2**) and diaqua (**5**) {$Ru(PTA)_4$} species occurs under these conditions.

Conversely, the treatment of **15** with 6 equiv. of PTA in methanol or acetone at room temperature afforded no product, but PTA was completely converted to PTAO within a few hours. When the reaction was performed in chloroform under reflux (no reaction occurred at room temperature), the observation of the precipitation of **2** in moderate yield implies that chloride abstraction from the solvent occurs. This finding suggests that cationic Ru^{II}–PTA species have a very high chloride affinity.

Compound **12** has the characteristics of a good precursor for the preparation of Ru^{II}–PTA derivatives, as it has the two dmso-*S* ligands that, in principle, might be replaced relatively easily by a chelating diimine. Indeed, we found that when **12** was treated with a slight excess of bpy in ethanol under reflux, the original pale yellow solution became progressively ruby red. A product of the same color, identified as *cis*,*cis*-$Ru(bpy)Cl_2(PTA)_2$ (**16**), was isolated in moderate-to-good yield (Scheme 5).

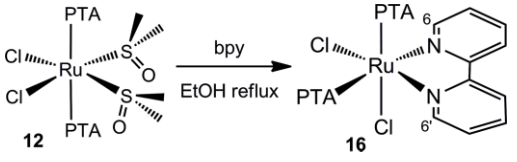

Scheme 5. Preparation of *cis*,*cis*-$Ru(bpy)Cl_2(PTA)_2$ (**16**) upon the treatment of *cis*,*cis*,*trans*-$RuCl_2(dmso\text{-}S)_2(PTA)_2$ (**12**) with bpy in ethanol under reflux.

Thus, the selective replacement of the two dimethyl sulfoxide ligands by bpy is accompanied by the concomitant isomerization to yield the less symmetrical all-*cis* product. Compound **16**, which is highly soluble in water, chloroform, and DMSO and moderately soluble in MeOH and EtOH, was characterized by NMR spectroscopy and mass spectrometry, and its X-ray structure was determined (Figure 5).

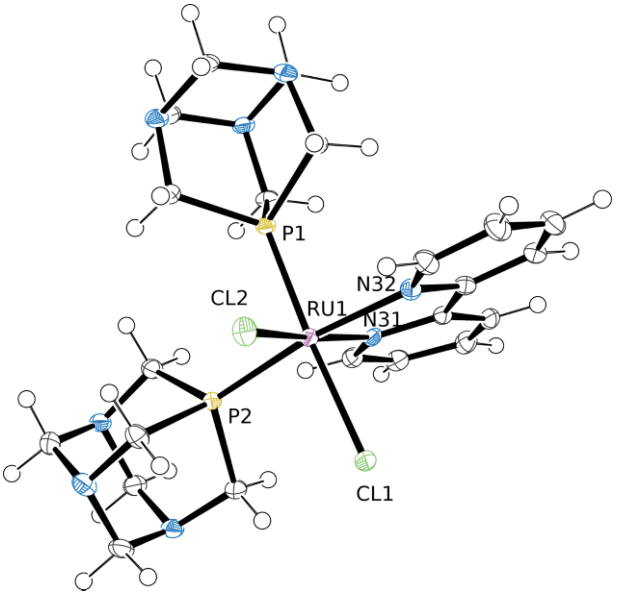

Figure 5. Molecular structure (50 % probability ellipsoids) of *cis*,*cis*-$Ru(bpy)Cl_2(PTA)_2$ (**16**). The three MeOH molecules of crystallization have been omitted for clarity.

In the ^1H NMR spectrum in $CDCl_3$, bpy presents eight well-resolved resonances (1 H each, Figure S24). As above, the most

deshielded doublet was assigned to 6-H (Scheme 5). The two inequivalent PTA ligands give four resolved resonances (6 H each, Figure 6), which are pairwise coupled in the H–H COSY spectrum (Figure S25). The two most upfield multiplets are attributed to the PTA ligand *trans* to the Cl ligand that falls into the shielding cone of the adjacent bpy ligand. The assignments were confirmed by a ^{1}H–^{31}P HMBC spectrum.

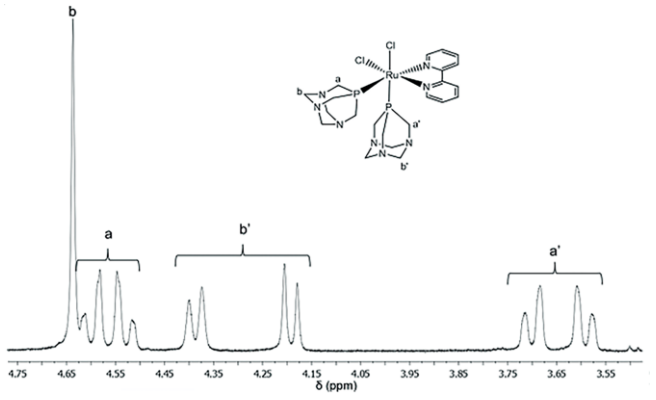

Figure 6. ^{1}H NMR spectrum (PTA region) of *cis*,*cis*-Ru(bpy)Cl_2(PTA)$_2$ (**16**) in $CDCl_3$. See the inset for the peak labels.

The ^{31}P NMR spectrum of **16** in D_2O (two doublets at δ = –7.0 and –31.9 ppm, $^{2}J_{P,P}$ = 37.7 Hz) is similar to that of **16** in $CDCl_3$ (Figure S28). However, whereas the shielded resonance is compatible with a P atom *trans* to a N atom, the other doublet falls in the region for a PTA ligand *trans* to an O atom (see, for example, the spectra of **2**$_{aq}$ and **10**$_{aq}$) rather than *trans* to a Cl ligand (expected at $\delta \approx -15$ ppm). Thus, we hypothesized that **16** in water undergoes rapid, quantitative, and selective release of the Cl ligand *trans* to PTA to afford *cis*,*cis*-[Ru(bpy)Cl(OH_2)(PTA)$_2$]$^{+}$ (**16**$_{aq}$, Scheme 6). This hypothesis is consistent with the following: (1) the larger *trans* influence of PTA compared with that of bpy, which is reflected by the solid-state data, according to which the Ru–Cl bond *trans* to PTA [2.4789(4) Å] is longer than that *trans* to bpy [2.4422(4) Å]; (2) the downfield-shifted resonance of 6-H implies that the adjacent Cl ligand remains bound to the ruthenium center.

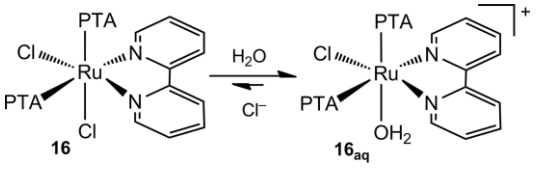

Scheme 6. Selective aquation of **16**.

Indeed, we found that the addition of aliquots of NaCl to the D_2O solution led to the progressive growth of a new set of resonances in the NMR spectra, attributed to intact **16**, at the expense of the original ones, which are, thus, attributed unambiguously to **16**$_{aq}$. An intermediate situation in the ^{31}P NMR spectrum is shown in Figure 7 (see Figure S29 for the ^{1}H NMR spectrum). As expected, the chemical shift of the new deshielded doublet in the ^{31}P NMR spectrum (δ = –12.7 ppm) is now in the region compatible with a P atom *trans* to a Cl ligand. The complete transformation of **16**$_{aq}$ to **16** upon the addition of excess NaCl (ca. 1 M) also induces a minor shift in the absorption maximum of the UV/Vis absorption spectrum from λ = 413 (**16**$_{aq}$) to 418 nm (**16**, Figure S38).

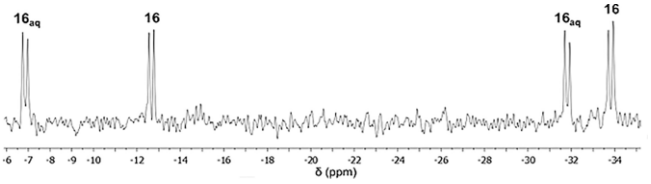

Figure 7. ^{31}P NMR spectrum of *cis*,*cis*-[Ru(bpy)Cl(OH_2)(PTA)$_2$]$^{+}$ (**16**$_{aq}$) in D_2O after the addition of an aliquot of NaCl (ca. 0.2 M) to afford a mixture of **16** and **16**$_{aq}$.

Similarly, the treatment of **12** with bpyAc in ethanol under reflux afforded *cis*,*cis*-Ru(bpyAc)Cl_2(PTA)$_2$ (**17**) as a nearly 1:1 mixture of the two stereoisomers **17a** (4-carboxylic acid *trans* to PTA) and **17b** (4-carboxylic acid *trans* to Cl, Scheme 7).

The spectroscopic features of **17a** and **17b** (Figures S30–S34) are quite similar, except for the bpyAc resonances in the ^{1}H NMR spectrum, for which twelve well-resolved signals (1 H each, six for each stereoisomer) were found in the aromatic region, plus two methyl singlets (3H each). The most deshielded doublet (δ = 9.58 ppm) was assigned to the 6-H proton in **17a** for the following reasons: (1) in free bpyAc, 6-H gives the most deshielded resonance (δ = 8.87 ppm vs. 8.57 ppm for 6′-H); (ii) in the complex, this proton is further deshielded by coordination and by the adjacent Cl ligand (see above). The second most downfield doublet was assigned to 6′-H in **17b**, in which it points towards the adjacent Cl atom. All other bpyAc resonances were then unambiguously assigned on the basis of the 2D H–H COSY and NOESY spectra. Particularly relevant were the cross-peaks between the CH_3 group (at the 4′-position) and the 3′-H singlets in the COSY spectrum and those between the singlets of 3-H and 3′-H in the NOESY spectrum. As for **16**, the dissolution of **17** in water results in the release of the Cl ligand *trans* to PTA to afford a mixture of **17a**$_{aq}$ and **17b**$_{aq}$, albeit at a slower rate.

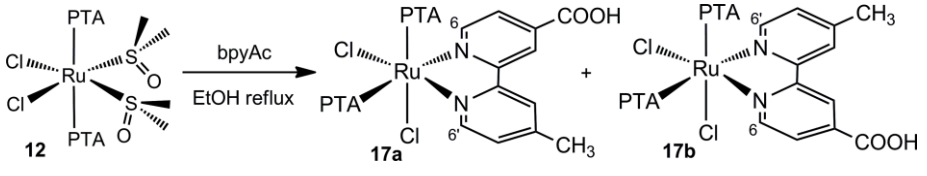

Scheme 7. Preparation of *cis*,*cis*-Ru(bpyAc)Cl_2(PTA)$_2$ (**17**) as a 50:50 mixture of the two stereoisomers **17a** and **17b**.

3. Conclusions

In this manuscript, we reported a thorough investigation of the neutral isomers *trans*- and *cis*-$RuCl_2(PTA)_4$ (**1** and **2**, respectively), including their unprecedented comprehensive NMR spectroscopy characterization (^1H, ^{13}C, and ^{31}P) both in D_2O and in $CDCl_3$ (Table 1).

The reactivity of **1** and **2** was basically unexplored. When warmed in a coordinating solvent such as DMSO or acetonitrile, the kinetic complex **1** isomerizes to the thermodynamically stable *cis* isomer **2**, as it does in water. The neutral intermediates *cis*,*mer*-$RuCl_2$(dmso-*S*)$(PTA)_3$ (**6**), *trans*,*mer*-$RuCl_2(CH_3CN)(PTA)_3$ (**7**), and *cis*,*mer*-$RuCl_2(CH_3CN)(PTA)_3$ (**8**) were isolated, albeit not in pure form. Most interestingly, by virtue of these results, we found that both **1** and **2** can be used as precursors of the $\{RuCl(PTA)_3\}^+$ fragment. They react with chelating diimines such as bpy in water under reflux through the selective replacement of one chlorido ligand and one PTA ligand to afford the two unprecedented isomeric derivatives *mer*-[Ru(bpy)Cl$(PTA)_3$]Cl (**9**) and *fac*-[Ru(bpy)Cl$(PTA)_3$]Cl (**10**), depending on the conditions. We are confident that the new insights provided by this work on **1** and **2** will be valuable, in particular, for those interested in the exploitation of these complexes and their derivatives as catalysts.

We also investigated the reactivity of the Ru^{II}–dmso complexes *cis*,*fac*-$RuCl_2$(dmso-*O*)(dmso-*S*)$_3$ (**11**), *trans*-$RuCl_2$(dmso-*S*)$_4$ (**13**), *cis*,*fac*-[RuCl(dmso-*O*)$_2$(dmso-*S*)$_3$][PF_6] (**14**), and *fac*-[Ru(dmso-*O*)$_3$(dmso-*S*)$_3$][CF_3SO_3]$_2$ (**15**) towards PTA. Expanding the results reported by Kathó and co-workers,[11] we found that PTA reacts rapidly with the neutral Ru–dmso precursors under mild conditions through the replacement of pairs of mutually *trans* dmso ligands with high selectivity. The replacement of both dmso ligands also occurs when PTA is in stoichiometric defect. Thus, **11** affords selectively *cis*,*cis*,*trans*-$RuCl_2$(dmso-*S*)$_2(PTA)_2$ (**12**), whereas **13** gives **1**. In both cases, no intermediates could be isolated or even detected. Conversely, no new cationic Ru^{II}–PTA complexes were obtained from **14** and **15**. We also found that the two dmso ligand of **12** can be replaced selectively by chelating diimines such as bpy and bpyAc. Nevertheless, the substitution is accompanied by isomerization, and the less symmetrical all-*cis* products *cis*,*cis*-Ru(bpy)$Cl_2(PTA)_2$ (**16**) and *cis*,*cis*-Ru(bpyAc)$Cl_2(PTA)_2$ (**17**, as a 50:50 mixture of the two stereoisomers **17a** and **17b**) were obtained. Thus, **12** is a promising precursor for the attachment of the highly water-solubilizing $\{RuCl_2(PTA)_2\}$ fragment to bidentate linkers.

In general, as anticipated, all of the neutral Ru–PTA complexes acquire the amphiphilic nature of PTA and are quite soluble both in organic solvents (e.g., chloroform) and in water. Perhaps counterintuitively, the solubility in water decreases upon protonation of the coordinated PTA ligand to such an extent that the addition of a strong mineral acid to an aqueous solution of a neutral Ru–PTA complex is often a convenient approach to obtain crystals of the corresponding charged PTAH derivative.

Finally, we established that the ^{31}P NMR resonance of a PTA ligand bound to a Ru^{II} center is largely independent on the solvent but is remarkably affected by the nature of the ligand in the *trans* position and, thus, it can be used as a diagnostic tool to establish the geometry of octahedral Ru–PTA complexes.[31] The typical chemical-shift regions as well as the corresponding interval for the Ru^{II}–P bond lengths are reported in Table 2. With the exception of the bis(hydride) complex *cis*-$RuH_2(PTA)_4$,[26,32] there is a rough correlation between the two parameters: as the Ru–P bond length increases, the ^{31}P NMR resonance shifts progressively to lower frequencies.

Table 2. Typical ^{31}P NMR chemical-shift intervals (Δ) and Ru–P bond lengths for PTA bound to octahedral Ru^{II} complexes as a function of the nature of the *trans* ligand.

Ligand *trans* to PTA	Δ ^{31}P [ppm][a]	Ru–P [Å]	Reference
OH_2/OH	–7 to –16	–	this work, ref.[2]
Cl	–20 to –26	2.232–2.283	this work, ref.[5b]
Br	–24 to –27	2.266–2.281	ref.[29]
S[b]	–30 to –45	2.280–2.318	ref.[13,21]
N[c]	–34 to –50	2.260–2.344	this work, ref.[15b,33–37]
H	–26.6[d]	2.299–2.300	ref.[26]
P[e]	–50 to –60	2.290–2.400	this work, ref.[2,5b,11,14,26,28,29]
C[f]	–68.4[d]	2.395(1)	ref.[38]

[a] For comparison, the singlet of free PTA falls at δ = –98.2 ppm in D_2O and at δ = –102.3 ppm in $CDCl_3$. [b] From [9]aneS3. [c] From imine or azole. [d] Only one example. [e] From PTA. [f] From cyclometalated 2-phenylpyridine.

Experimental Section

Materials: All chemicals were purchased from Sigma–Aldrich and used as received. Solvents were of reagent grade. The precursors *trans*-$RuCl_2(PTA)_4$ (**1**),[5] *cis*,*fac*-$RuCl_2$(dmso-*O*)(dmso-*S*)$_3$ (**11**),[39] *trans*-$RuCl_2$(dmso-*S*)$_4$ (**13**),[39] *cis*,*fac*-[RuCl(dmso-*O*)$_2$(dmso-*S*)$_3$][PF_6] (**14**),[40] *fac*-[Ru(dmso-*O*)$_3$(dmso-*S*)$_3$](CF_3SO_3)$_2$ (**15**),[41] and the ligand bpyAc[42] were synthesized as described in the literature.

Instrumental Methods: 1D [^1H (400 or 500 MHz), ^{13}C (125.7 MHz), and ^{31}P (161 or 202 MHz)] and 2D (^1H–^1H COSY, ^1H–^{13}C HSQC, ^{31}P–^{31}P COSY, ^1H–^{31}P HMBC, and ^1H–^1H NOESY) NMR spectra were recorded at room temperature with a JEOL Eclipse 400FT spectrometer or a Varian 500 spectrometer. The ^1H and ^{13}C chemical shifts were referenced to the peak of the residual non-deuterated solvent (δ = 7.26 ppm and δ = 77.16 ppm for $CDCl_3$) or measured relative to the internal standard 4,4-dimethyl-4-silapentane-1-sulfonic acid (DSS, δ = 0.00 ppm) for D_2O. The ^{31}P chemical shifts were measured relative to external 85 % H_3PO_4 at δ = 0.00 ppm. The ^1H–^{31}P HMBC spectra were recorded by using the standard sequence HMBCAD with the Varian 500 spectrometer with a coupling constant (^2J) of 5–10 Hz. The ESI mass spectra were collected in the positive mode with a Perkin–Elmer APII spectrometer at 5600 eV. The UV/Vis spectra were obtained with an Agilent Cary 60 spectrophotometer with 1.0 cm path-length quartz cuvettes (3.0 mL). The elemental analyses were performed in the Department of Chemistry of the University of Bologna. A home-made light-emitting diode (LED) apparatus, described elsewhere,[29] was used for the photochemical reactions.

X-ray Diffraction: Data collections were performed at the X-ray diffraction beamline (XRD1) of the Elettra Synchrotron of Trieste (Italy).[43] Details are reported in the Supporting Information.[44–49]

Identification of the Complexes: For all complexes, the assignment of ^1H NMR PTA resonances was achieved through ^1H–^1H COSY and ^1H–^{13}C HSQC 2D NMR spectroscopy (Supporting Information). The assignment of the ^{31}P NMR resonances was consistent with the multiplicity and integration of the peaks as well as with the ^{31}P–^{31}P COSY spectra.

***cis*-RuCl$_2$(PTA)$_4$ (2):** A procedure similar to that reported by Romerosa and co-workers,[27] that is, the photoisomerization of **1** in aqueous solution, was followed. Complex **1** (50.0 mg, 0.062 mmol) was dissolved in water (5 mL) and irradiated with blue light (λ = 470 nm, 40 mW) for 1 h, during which the orange solution turned yellow. The complete removal of the solvent by rotary evaporation afforded pure **1** as a yellow solid (yield: 48.0 mg, 96 %). $C_{24}H_{48}Cl_2N_{12}P_4Ru$ (800.57): calcd. C 36.01, H 6.04, N 20.99; found C 36.12, H 6.19, N 21.12. ^{1}H NMR (D_2O + NaCl): δ = 4.65 (m, 24 H, NCH_2N), 4.47 (br. s, 12 H, NCH_2P, mutually *trans* PTAs), 4.14 (br. s, 12 H, NCH_2P, PTA *trans* to Cl) ppm. ^{31}P NMR (D_2O + NaCl): δ = –21.6 (t, $^2J_{P,P}$ = 28.5 Hz, 2 P, PTA *trans* to Cl), –57.6 (t, 2 P, mutually *trans* PTAs) ppm. ^{1}H NMR ($CDCl_3$): δ = 4.48 (m, 24 H, NCH_2N), 4.47 (br. s, 12 H, NCH_2P, mutually *trans* PTAs), 4.04 (br. s, 12 H, NCH_2P, PTA *trans* to Cl) ppm. ^{13}C NMR (HSQC, $CDCl_3$): δ = 73.1 (NCH_2P), 58.7 (NCH_2N mutually *trans* PTAs), 54.8 (NCH_2P PTAs *trans* to Cl) ppm. ^{31}P NMR ($CDCl_3$): δ = –24.1 (t, $^2J_{P,P}$ = 28.6 Hz, 2 P, PTAs *trans* to Cl), –59.4 (t, 2 P, mutually *trans* PTAs) ppm. ESI MS: *m*/*z* = 765.1 [M – Cl]$^+$, 608.2 [M – Cl – PTA]$^+$. UV/Vis ($CHCl_3$): λ_{max} (ε, L mol^{-1} cm^{-1}) = 344 (1022) nm.

***cis*-[RuCl(OH$_2$)(PTA)$_4$][PF$_6$]·CH$_3$OH (2_{aq}):** [RuCl(dmso)$_5$][PF$_6$] (38.3 mg, 0.057 mmol) was dissolved in methanol (10 mL). PTA (44.8 mg, 0.29 mmol, 5 equiv.) was added, and the solution was left to stand overnight in the dark. Yellow crystals formed slowly from the concentrated solution (5 mL). Some crystals were selected for X-ray diffraction, and the others were collected by filtration, washed with diethyl ether, and dried in vacuo (yield: 22.8 mg, 42 %). $C_{24}H_{50}ClF_6N_{12}OP_5Ru$·$CH_3OH$ (960.15): calcd. C 31.27, H 5.67, N 17.51; found C 31.47, H 5.83, N 17.70. ^{1}H NMR (D_2O): δ = 4.59 (m, 24 H, NCH_2N), 4.26 (d, 12 H, NCH_2P), 4.11 (s, 6 H, NCH_2P), 3.97 (s, 6 H, NCH_2P), 3.34 ppm (s, 3 H, MeOH free). ^{31}P NMR (D_2O): δ = –12.7 (dt, $^2J_{A,M}$ = 30.3, $^2J_{A,X}$ = 34.8 Hz, 1 P, PTA *trans* to OH$_2$), –22.7 (dt, $^2J_{X,M}$ = 26.1, $^2J_{X,A}$ = 34.8 Hz, 1 P, PTA *trans* to Cl), –52.6 (dd, $^2J_{M,X}$ = 26.1, $^2J_{M,A}$ = 30.3 Hz, 2 P, mutually *trans* PTAs), –143.2 (septet, 1 P, PF$_6$) ppm. ESI MS: *m*/*z* = 765.1 [M – H$_2$O]$^+$.

***cis*,*mer*-RuCl$_2$(dmso-*S*)(PTA)$_3$ (6):** Complex **1** (30.0 mg, 0.038 mmol) was partially dissolved in DMSO (1 mL), and the mixture was warmed to 70 °C whilst stirring. After 2 h of reaction, the residual unreacted **1** was removed by filtration. The dropwise addition of acetone to the mother liquor induced the formation of a pale yellow precipitate within 24 h. The precipitate was removed by filtration, washed with diethyl ether, and dried in vacuo. According to the ^{1}H and ^{31}P NMR spectra, the product was a mixture of **6** and **2** in an approximate ration of 40:60 (yield: 9 mg, 33 %). ^{1}H NMR ($CDCl_3$): δ = 3.20 (s, 6H, dmso-*S*) ppm; in the PTA region, the resonances of **2** and **6** overlap to such an extent that those of **6** could not be distinguished. ^{31}P NMR ($CDCl_3$): δ = –25.6 (t, $^2J_{P,P}$ = 27.9 Hz, 1 P, PTA *trans* to Cl), –61.0 (d, 2 P, mutually *trans* PTAs) ppm.

***trans*,*mer*-RuCl$_2$(CH$_3$CN)(PTA)$_3$ (7) and *cis*,*mer*-RuCl$_2$(CH$_3$CN)(PTA)$_3$ (8):** Complex **1** (60.0 mg, 0.075 mmol) was partially dissolved in acetonitrile (8 mL), and the mixture was heated under reflux for 2 h. Upon heating, **1** dissolved completely, the originally yellow solution became progressively paler, and a pale yellow solid began to form after ca. 1 h. After cooling to room temperature, the product was collected by filtration, washed with acetonitrile and diethyl ether, and dried in vacuo. According to the ^{1}H and ^{31}P NMR spectra, the product was a mixture of **7**, **8**, and **1** in an approximate ratio of 68:17:15 (yield: 15 mg, 29 %). ^{1}H NMR ($CDCl_3$): complexes **7** and **8**: δ = 4.45 (m, NCH_2N), 4.04 (br. s, NCH_2P), 2.46 (s, 3H, CH_3CN of **8**), 2.30 (s, 3H, CH_3CN of **7**) ppm; it was not possible to distinguish the PTA resonances of **7** and **8**. ^{31}P NMR ($CDCl_3$): complex **7**: δ = –16.1 (t, 1 P, $^2J_{P,P}$ = 28.5 Hz, PTA *trans* to CH$_3$CN), –53.3 (d, 2 P, mutually *trans* PTAs) ppm; complex **8**: δ = –24.0 (t, $^2J_{P,P}$ = 37.2 Hz, 1 P, PTA *trans* to Cl), –54.3 (d, 2 P, mutually *trans* PTAs) ppm.

***mer*-[Ru(bpy)Cl(PTA)$_3$]Cl (9):** Complex **1** (40.0 mg, 0.050 mmol) was dissolved in water (5 mL). 2,2′-Bipyridine (8.2 mg, 0.050 mmol) was added, and the light-protected mixture was heated under reflux for 1 h. The yellow solution turned rapidly orange. The solvent was removed by rotary evaporation to afford a yellow solid that was an approximately equimolar mixture of free PTA and **9** with PTAO as an impurity (less than 5 % of PTA) on the basis of the ^{1}H and ^{31}P NMR spectra. X-ray quality crystals of **9** were obtained by the slow diffusion of acetone into a water solution of the complex. $C_{28}H_{44}Cl_2N_{11}P_3Ru$·$6H_2O$ (907.70): calcd. C 37.05, H 6.22, N 16.97; found C 36.87, H 6.03, N 16.87. Larger amounts of pure complex for NMR spectroscopy characterization were obtained of the PF$_6$ salt (**9**PF$_6$): the raw material (48.1 mg) was dissolved in water (1 mL) and a solution (1 mL) of NaPF$_6$ (12.5 mg, 0.075 mmol) was added. The yellow crystals that formed in a few hours were collected by filtration and dried in vacuo (yield: 28.1 mg, 62 %). The product was pure **9**PF$_6$ according to the ^{1}H and ^{31}P NMR spectra. ^{1}H NMR (D_2O): δ = 9.45 (d, 1 H, 6-H), 8.65 (d, 1 H, 3-H), 8.55 (d, 1 H, 3′-H), 8.41 (m, 2 H, 4-H + 6′-H), 8.18 (t, 1 H, 4′-H), 7.94 (t, 1 H, 5-H), 7.58 (t, 1 H, 5′-H), 4.93, 4.85 (AB q, $J_{A,B}$ = 13.1 Hz, 6 H, NCH_2N, PTA *trans* to N), 4.52 (br. s, 6 H, NCH_2P, PTA *trans* to N), 4.54, 4.45 (AB q, $J_{A,B}$ = 13.9 Hz, 12 H, NCH_2N, mutually *trans* PTAs), 3.72 (br. s, 12 H, NCH_2P, mutually *trans* PTAs) ppm. ^{13}C NMR (partial, HSQC, D_2O): δ = 156.2 (C-6′), 150.7 (C-6), 146.8 (C-4), 138.9 (C-4′), 128.2 (C-5′), 127.3 (C-5), 125.6 (C-3′), 124.9 (C-3), 70.7 (NCH_2N, PTA *trans* to N), 70.5 (NCH_2N, mutually *trans* PTAs), 52.2 (NCH_2P, PTA *trans* to N), 46.6 (NCH_2P, mutually *trans* PTAs) ppm. ^{31}P NMR (D_2O): δ = –30.2 (t, $^2J_{P,P}$ = 32.8 Hz, 1 P, PTA *trans* to N), –47.6 (d, 2 P, mutually *trans* PTAs), –144.4 (septet, PF$_6$) ppm. ESI MS: *m*/*z* = 764.2 [M]$^+$, 607.2 [M – PTA]$^+$. UV/Vis (H_2O): λ_{max} (ε, L mol^{-1} cm^{-1}) = 390 (1310) nm.

***fac*-[Ru(bpy)Cl(PTA)$_3$]Cl (10):** Complex **2** (45.0 mg, 0.056 mmol) was dissolved in water (8 mL). 2,2′-Bipyridine (43.9 mg, 0.280 mmol) and $AgNO_3$ (9.6 mg, 0.056 mmol) were added, and the light-protected mixture was heated under reflux for 1 h. The yellow solution turned rapidly orange, and a grey precipitate of AgCl formed. The mixture was filtered through a pad of Celite, and the solvent was removed from the clear solution by rotary evaporation to afford a yellow solid, which, according to the ^{1}H and ^{31}P NMR spectra, was a mixture of **9** and **10** in a 1:7 ratio. No residual **2** was present. The pure *fac* isomer for full characterization was obtained as a PF$_6$ salt (**10**PF$_6$): the raw mixture (87.3 mg) was dissolved in water (1 mL), and a solution (1 mL) of NaPF$_6$ (18.6 mg, 0.11 mmol) was added. The yellow microcrystalline solid that formed within a few hours at room temperature was collected by filtration, washed with cold water, and dried in vacuo (yield: 14.1 mg, 31 %). The product was pure **10**PF$_6$ according to the ^{1}H and ^{31}P NMR spectra. Low-quality single crystals of fully protonated **10**, as *fac*-[Ru(bpy)Cl(PTAH)$_3$][0.5Cl]-[3.5ClO$_4$], were obtained through the addition of a 0.5 M solution of $HClO_4$ to a water solution of the complex and used for X-ray diffraction analysis. Complex **10**PF$_6$: $C_{28}H_{44}ClF_6N_{11}P_4Ru$ (909.13): calcd. C 36.99, H 4.88, N 16.95; found C 37.18, H 4.90, N 17.03. ^{1}H NMR (D_2O + NaCl): δ = 8.99 (br. s, 2 H, 6-H), 8.54 (d, 2 H, 3-H), 8.29 (t, 2 H, 4-H), 7.80 (t, 2 H, 5-H), 4.65 (m, partially overlapped by the water signal, 12 H, NCH_2N, PTA *trans* to N), 4.49 (m, partially overlapped by the singlet at 4.44, 6 H, NCH_2N, PTA *trans* to Cl), 4.44 (s, 12 H, NCH_2P, PTA *trans* to N), 3.88 (s, 6 H, NCH_2P, PTA *trans* to Cl) ppm. ^{13}C NMR (partial, HSQC, D_2O): δ = 154.5 (C-6), 140.3 (C-4), 126.5 (C-5), 124.7 (C-3), 70.7 (NCH_2N, PTA *trans* to Cl), 70.5 (NCH_2N, PTA *trans* to N), 52.2 (NCH_2P, PTA *trans* to Cl), 46.6 (NCH_2P, PTA *trans* to N) ppm. ^{31}P NMR (D_2O): δ = –24.3 (t, $^2J_{P,P}$ = 29.2 Hz, 1 P, PTA *trans* to Cl), –43.1 (d, 2 P, PTA *trans* to N), –144.4 (septet, 1 P, PF$_6$) ppm. Complex **10**$_{aq}$: ^{1}H NMR (D_2O): δ = 8.95 (br. s, 2 H, 6-H), 8.58 (d, 2 H, 3-H), 8.33 (t, 2 H, 4-H), 7.83 (t, 2 H, 5-H), 4.65 (m, 12H,

NCH_2N), 4.46 (s, 12H, NCH_2P), 4.43 (m, 6H, NCH_2N, PTA *trans* to OH_2), 3.84 (s, 6H, NCH_2P, PTA *trans* to OH_2) ppm; it was not possible to distinguish the PTA resonances of **10** and $\mathbf{10}_{aq}$. ^{31}P NMR (D_2O): δ = –17.7 (t, 1 P, $^2J_{P,P}$ = 30.2 Hz, PTA *trans* to OH_2), –43.5 (d, 2 P, PTA *trans* to N), –144.4 (septet, 1 P, PF_6) ppm. ESI MS: *m/z* = 764.2 $[M]^+$, 607.2 $[M – PTA]^+$. UV/Vis (H_2O): λ_{max} (ε, L mol^{-1} cm^{-1}) = 385 (2385) nm.

***cis,cis,trans*-RuCl$_2$(dmso-*S*)$_2$(PTA)$_2$ (12):** A different procedure to that reported by Kathó and co-workers was followed.[11] Complex **11** (340 mg, 0.70 mmol) was partially dissolved in methanol (5 mL). A solution of PTA (220 mg, 1.4 mmol) in methanol (10 mL) was added dropwise over 15 min. A pale yellow solid began to form after a few minutes. The reaction was left to stand overnight, and the product was collected by filtration, washed with methanol and diethyl ether, and dried in vacuo (yield: 357 mg, 80 %). According to the ^{1}H and ^{31}P NMR spectra, the product was pure **12**. X-ray quality crystals of **12** were obtained by the slow diffusion of diethyl ether into a methanol solution of the complex. $C_{16}H_{36}N_6Cl_2P_2S_2O_5Ru$ (642.55): calcd. C 29.91, H 5.65, N 13.08; found C 29.99, H 5.60, N 13.15. ^{1}H NMR (D_2O): δ = 4.51 (br. s, 12 H, NCH_2N), 4.32 (br. s, 12 H, NCH_2P), 3.38 (s, 12 H, dmso-*S*) ppm. ^{31}P NMR (D_2O): δ = –57.9 (s) ppm. ^{1}H NMR ($CDCl_3$): δ = 4.52, 4.47 (AB q, $J_{A,B}$ = 13.0 Hz, 12 H, NCH_2N), 4.41 (br. s, 12 H, NCH_2P), 3.32 (s, 12 H, dmso-*S*) ppm. ^{13}C NMR ($CDCl_3$): δ = 73.1 (NCH_2N), 51.3 (NCH_2P), 51.1 (dmso-*S*) ppm. ^{31}P NMR ($CDCl_3$): δ = –63.5 (s) ppm. ESI MS: *m/z* = 643.0 $[M]^+$.

***cis,cis*-Ru(bpy)Cl$_2$(PTA)$_2$ (16):** Complex **12** (70.0 mg, 0.109 mmol) was partially dissolved in ethanol (10 mL). 2,2′-Bipyridine (34.0 mg, 0.218 mmol) was added, and the mixture was heated under reflux for 6 h. The clear solution obtained gradually become ruby red upon warming, and a precipitate of the same color began to form after 4 h. The mixture was concentrated to ca. 3 mL and left to stand overnight at room temperature, and the precipitate was collected by filtration, washed with diethyl ether, and dried in vacuo (yield: 42.0 mg, 54 %). According to the ^{1}H and ^{31}P NMR spectra, the product was pure **16**. X-ray quality crystals of **16** were obtained by the slow diffusion of diethyl ether into a methanol solution of the complex. $C_{22}H_{32}Cl_2N_8P_2Ru$ (642.46): calcd. C 41.13, H 5.02, N 17.44; found C 41.16, H 5.00, N 17.45. ^{1}H NMR ($CDCl_3$): δ = 9.88 (d, 1 H, 6-H bpy), 8.55 (d, 1 H, 6′-H bpy), 8.10 (d, 1 H, 3-H bpy), 8.04 (d, 1 H, 3′-H bpy), 7.95 (t, 1 H, 4-H bpy), 7.78 (t, 1 H, 4′-H bpy), 7.58 (t, 1 H, 5-H bpy), 7.20 (t, 1 H, 5′-H bpy), 4.64 (s, 6 H, NCH_2N, PTA *trans* to N), 4.60, 4.53 (AB q, $J_{A,B}$ = 15.0 Hz, 6 H, NCH_2P, PTA *trans* to N), 4.39, 4.19 (AB q, $J_{A,B}$ = 13.0 Hz, 6 H, NCH_2N, PTA *trans* to Cl), 3.70, 3.59 (AB q, $J_{A,B}$ = 15.1 Hz, 6 H, NCH_2P, PTA *trans* to Cl) ppm. ^{13}C NMR (partial, HSQC, $CDCl_3$): δ = 156.7 (C-6′), 151.1 (C-6), 136.9 (C-4), 135.2 (C-4′), 125.8 (C-5), 125.2 (C-5′), 122.9 (C-3′), 121.7 (C-3), 73.31 (NCH_2N, PTA *trans* to N), 72.0 (NCH_2N, PTA *trans* to Cl), 54.0 (NCH_2P, PTA *trans* to N), 53.2 (NCH_2P, PTA *trans* to Cl) ppm. ^{31}P NMR ($CDCl_3$): δ = –21.6 (d, $^2J_{P,P}$ = 34.4 Hz, 1 P, PTA *trans* to Cl), –36.2 (d, 1 P, *trans* to N) ppm. ^{1}H NMR (D_2O): complex $\mathbf{16}_{aq}$: δ = 9.51 (d, 1 H, 6-H bpy), 8.53 (d, 1 H, 6′-H bpy), 8.49 (d, 1 H, 3-H bpy), 8.42 (d, 1 H, 3′-H bpy), 8.27 (t, 1 H, 4-H bpy), 8.09 (t, 1 H, 4′-H bpy), 7.80 (t, 1 H, 5-H bpy), 7.50 (t, 1 H, 5′-H bpy), 4.66 (s, 6 H, NCH_2N, PTA *trans* to N), 4.45 (s, 6H, NCH_2P, PTA *trans* to N), 4.38, 4.27 (AB q, 6H, $J_{A,B}$ = 13.3 Hz, NCH_2N, PTA *trans* to OH_2), 3.66 (m, 6H, NCH_2P, PTA *trans* to OH_2) ppm. ^{31}P NMR (D_2O): δ = –7.0 (d, $^2J_{P,P}$ = 37.7 Hz, PTA *trans* to OH_2), –31.9 (d, PTA *trans* to N) ppm. ^{1}H NMR: (D_2O + NaCl): complex **16**: δ = 9.45 (d, 1 H, 6-H bpy), 8.55 (m, 1 H, 6′-H bpy), 8.44 (d, 2 H, 3-H and 3′-H), 8.22 (t, 1 H, 4-H bpy), 8.02 (t, 1 H, 4′-H bpy), 7.75 (t, 1 H, 5-H bpy), 7.45 (t, 1 H, 5′-H bpy), 4.38 (m, 12H, NCH_2N), 3.65 (m, 12H, NCH_2P) ppm; it was not possible to distinguish the PTA resonances of **16** and $\mathbf{16}_{aq}$. ^{31}P NMR (D_2O + NaCl): δ = –12.7 (d, $^2J_{P,P}$ = 37.1 Hz, 1 P, PTA *trans* to Cl), –33.8 (d, 1 P, PTA *trans* to N) ppm. ESI MS: *m/z* = 607.0 $[M – Cl]^+$. UV/Vis (H_2O): λ_{max} (ε, L mol^{-1} cm^{-1}) = 412 (2839) nm.

***cis,cis*-Ru(bpyAc)Cl$_2$(PTA)$_2$ (17):** Complex **12** (50.0 mg, 0.078 mmol) was partially dissolved in ethanol (15 mL). 4′-Methyl-2,2′-bipyridine-4-carboxylic acid (bpyAc, 33.4 mg, 0.156 mmol) was added, and the mixture was heated under reflux for 6 h. The clear solution obtained gradually became deep red upon warming. As the solution cooled to room temperature, a red powder precipitated. The red powder was collected by filtration, washed with ethanol and diethyl ether, and dried in vacuo (yield: 20.0 mg, 37 %). According to the ^{1}H and ^{31}P NMR spectra, the product was pure **17**, as a nearly equimolar mixture of the two stereoisomers **17a** and **17b**. $C_{24}H_{34}Cl_2N_8O_2P_2Ru$ (700.5): calcd. C 41.15, H 4.39, N 16.00; found C 41.05, H 4.33, N 15.95. ^{1}H NMR (D_2O): complex $\mathbf{17}_{aq}$: δ = 9.58 (d, 1 H, 6-H $\mathbf{17a}_{aq}$), 9.31 (d, 1 H, 6′-H $\mathbf{17b}_{aq}$), 8.74 (s, 1 H, 3-H $\mathbf{17a}_{aq}$), 8.67 (s, 1 H, 3-H $\mathbf{17b}_{aq}$), 8.57 (d, 1 H, 6-H $\mathbf{17b}_{aq}$), 8.42 (s, 1 H, 3′-H $\mathbf{17b}_{aq}$), 8.36 (s, 1 H, 3′-H $\mathbf{17a}_{aq}$), 8.32 (d, 1 H, 6′-H $\mathbf{17a}_{aq}$), 8.06 (d, 1 H, 5-H $\mathbf{17a}_{aq}$), 7.76 (d, 1 H, 5-H $\mathbf{17b}_{aq}$), 7.68 (d, 1 H, 5′-H $\mathbf{17b}_{aq}$), 7.39 (d, 1 H, 5′-H $\mathbf{17a}_{aq}$), 4.84 (br. s, 12 H, NCH_2N, PTA *trans* to N), 4.54 (br. s, 12 H, NCH_2P, PTA *trans* to N), 4.43 (m, 12 H, NCH_2N, PTA *trans* to OH_2), 3.77, 3.72 (AB q, 12 H, NCH_2P, $J_{A,B}$ = 14.7 Hz, PTA *trans* to OH_2), 2.64 (s, 3H, CH_3 $\mathbf{17b}_{aq}$), 2.56 (s, 3 H, CH_3 $\mathbf{17a}_{aq}$) ppm; the PTA resonances of $\mathbf{17a}_{aq}$ and $\mathbf{17b}_{aq}$ overlapped and could not be distinguished. ^{13}C NMR (partial, HSQC, D_2O): complex $\mathbf{17}_{aq}$: δ = 157.7 (C-6 $\mathbf{17b}_{aq}$), 156.4 (C-6′ $\mathbf{17a}_{aq}$), 150.7 (C-6 $\mathbf{17a}_{aq}$), 149.2 (C-6′ $\mathbf{17b}_{aq}$), 128.3 (C-5′ $\mathbf{17a}_{aq}$), 127.8 (C-5′ $\mathbf{17b}_{aq}$), 125.5 (C-5 $\mathbf{17b}_{aq}$), 125.1 (C-5 $\mathbf{17a}_{aq}$), 124.7 (C-3′ $\mathbf{17b}_{aq}$), 123.1 (C-3 $\mathbf{17b}_{aq}$), 122.5 (C-3 $\mathbf{17a}_{aq}$), 125.7 (C-3′ $\mathbf{17a}_{aq}$), 70.5 (NCH_2N, PTA *trans* to N), 70.5 (NCH_2N PTA *trans* to OH_2), 49.9 (NCH_2P, PTA *trans* to OH_2), 49.5 (NCH_2P, PTA *trans* to N), 21.0 (CH_3 $\mathbf{17b}_{aq}$), 20.0 (CH_3 $\mathbf{17a}_{aq}$) ppm; the PTA resonances of $\mathbf{17a}_{aq}$ and $\mathbf{17b}_{aq}$ overlapped and could not be distinguished. ^{31}P NMR (D_2O): complex $\mathbf{17}_{aq}$: δ = –4.0 (m, 4 P, PTA *trans* to OH_2), –26.0 (m, 4 P, PTA *trans* to N) ppm. ^{31}P NMR (D_2O + NaCl): complex **17**: δ = –9.5 (m, 4 P, PTA *trans* to Cl), –25.4 (m, 4 P, PTA *trans* to N) ppm. ESI MS: *m/z* = 665.2 $[M – Cl]^+$. UV/Vis (H_2O): λ_{max} (ε, L mol^{-1} cm^{-1}) = 412 (1615) nm.

CCDC 1449210 (for **9**), 1449211 (for **10**), 1449212 (for **12**), and 1449213 (for **16**) contain the supplementary crystallographic data for this paper. These data can be obtained free of charge from The Cambridge Crystallographic Data Centre.

Acknowledgments

Financial support from the Italian Ministero dell'Università e della Ricerca (MIUR) (PRIN 20085ZXFEE and FIRB RBAP11C58Y "NanoSolar"), the University of Trieste (FRA2015, grants to G. B. and E. A.; FRA2014, grant to E. I.), and Fondazione Beneficentia Stiftung is gratefully acknowledged. The authors wish to thank BASF Italia, Srl for a donation of hydrated ruthenium chloride.

Keywords: Synthesis design · Ruthenium · P ligands · Ligand effects · Water solubility

[1] a) D. J. Daigle, A. B. Pepperman Jr., S. L. Vail, *J. Heterocycl. Chem.* **1974**, *11*, 407–408; b) D. J. Daigle, *Inorg. Synth.* **1998**, *32*, 40–45.
[2] J. Kovács, F. Joó, A. Bényei, G. Laurenczy, *Dalton Trans.* **2004**, 2336–2340.
[3] a) A. D. Phillips, L. Gonsalvi, A. Romerosa, F. Vizza, M. Peruzzini, *Coord. Chem. Rev.* **2004**, *248*, 955–993; b) J. Bravo, S. Bolaño, L. Gonsalvi, M. Peruzzini, *Coord. Chem. Rev.* **2010**, *254*, 555–607.
[4] For a recent review, see: P. Crochet, V. Cadierno, *Dalton Trans.* **2014**, *43*, 12447–12462.

[5] a) D. J. Darensbourg, F. Joó, M. Kannisto, A. Katho, J. H. Reibenspies, *Organometallics* **1992**, *11*, 1990–1993; b) D. J. Darensbourg, F. Joó, M. Kannisto, A. Kathó, J. H. Reibenspies, D. J. Daigle, *Inorg. Chem.* **1994**, *33*, 200–208.
[6] a) G. Laurenczy, F. Joó, L. Nádasdi, J. Elek, *Chem. Commun.* **1999**, 971–972; b) G. Laurenczy, F. Joó, L. Nádasdi, *Inorg. Chem.* **2000**, *39*, 5083–5088; c) G. Laurenczy, F. Joó, L. Nádasdi, *High Pressure Res.* **2000**, *18*, 251–255; d) G. Kovács, L. Nádasdi, G. Laurenczy, F. Joó, *Green Chem.* **2003**, *5*, 213–217.
[7] W.-C. Lee, B. J. Frost, *Green Chem.* **2012**, *14*, 62–66.
[8] D. N. Akbayeva, L. Gonsalvi, W. Oberhauser, M. Peruzzini, F. Vizza, P. Brueggeller, A. Romerosa, G. Sava, A. Bergamo, *Chem. Commun.* **2003**, 264–265.
[9] G. Laurenczy, S. Jedner, E. Alessio, P. J. Dyson, *Inorg. Chem. Commun.* **2007**, *10*, 558–562.
[10] C. A. Mebi, R. P. Nair, B. J. Frost, *Organometallics* **2007**, *26*, 429–438.
[11] A. Udvardy, A. C. Bényei, Á. Kathó, *J. Organomet. Chem.* **2012**, *717*, 116–122.
[12] a) C. S. Allardyce, P. J. Dyson, D. J. Ellis, S. L. Heath, *Chem. Commun.* **2001**, 1396–1397; b) C. Scolaro, A. Bergamo, L. Brescacin, R. Delfino, M. Cocchietto, G. Laurenczy, T. J. Geldbach, G. Sava, P. J. Dyson, *J. Med. Chem.* **2005**, *48*, 4161–4171; c) P. J. Dyson, G. Sava, *Dalton Trans.* **2006**, 1929–1933; d) P. J. Dyson, *Chimia* **2007**, *61*, 698–703; e) A. Bergamo, A. Masi, P. J. Dyson, G. Sava, *Int. J. Oncol.* **2008**, *33*, 1281–1289; f) W. H. Ang, A. Casini, G. Sava, P. J. Dyson, *J. Organomet. Chem.* **2011**, *696*, 989–998; g) C. M. Clavel, E. Paunescu, P. Nowak-Sliwinska, A. W. Griffioen, R. Scopelliti, P. J. Dyson, *J. Med. Chem.* **2015**, *58*, 3356–3365; h) M. V. Babak, S. M. Meier, K. V. M. Huber, J. Reynisson, A. A. Legin, M. A. Jakupec, A. Roller, A. Stukalov, M. Gridling, K. L. Bennett, J. Colinge, W. Berger, P. J. Dyson, G. Superti-Furga, B. K. Keppler, C. G. Hartinger, *Chem. Sci.* **2015**, *6*, 2449–2456; i) A. Weiss, X. Ding, J. R. van Beijnum, I. Wong, T. J. Wong, R. H. Berndsen, O. Dormond, M. Dallinga, L. Shen, R. O. Schlingemann, R. Pili, C.-M. Ho, P. J. Dyson, H. van den Bergh, A. W. Griffioen, P. Nowak-Sliwinska, *Angiogenesis* **2015**, *18*, 233–244; j) B. S. Murray, M. V. Babak, C. G. Hartinger, P. J. Dyson, *Coord. Chem. Rev.* **2016**, *306*, 86–114.
[13] B. Serli, E. Zangrando, T. Gianferrara, C. Scolaro, P. J. Dyson, A. Bergamo, E. Alessio, *Eur. J. Inorg. Chem.* **2005**, 3423–3434.
[14] S. Grguric-Sipka, C. R. Kowol, S.-M. Valiahdi, R. Eichinger, M. A. Jakupec, A. Roller, S. Shova, V. B. Arion, B. K. Keppler, *Eur. J. Inorg. Chem.* **2007**, 2870–2878.
[15] a) A. García-Fernández, J. Díez, Á. Manteca, J. Sánchez, R. García-Navas, B. G. Sierra, F. Mollinedo, M. Pilar Gamasa, E. Lastra, *Dalton Trans.* **2010**, *39*, 10186–10196; b) E. Menéndez-Pedregal, J. Díez, Á. Manteca, J. Sánchez, A. C. Bento, R. García-Navas, F. Mollinedo, M. Pilar Gamasa, E. Lastra, *Dalton Trans.* **2013**, *42*, 13955–13967.
[16] R. Pettinari, F. Marchetti, F. Condello, C. Pettinari, G. Lupidi, R. Scopelliti, S. Mukhopadhyay, T. Riedel, P. J. Dyson, *Organometallics* **2014**, *33*, 3709–3715.
[17] S. Seršen, J. Kljun, K. Kryeziu, R. Panchuk, B. Alte, W. Körner, P. Heffeter, W. Berger, I. Turel, *J. Med. Chem.* **2015**, *58*, 3984–3996.
[18] a) E. Iengo, B. Milani, E. Zangrando, S. Geremia, E. Alessio, *Angew. Chem. Int. Ed.* **2000**, *39*, 1096–1099; *Angew. Chem.* **2000**, *112*, 1138; b) E. Iengo, E. Zangrando, R. Minatel, E. Alessio, *J. Am. Chem. Soc.* **2002**, *124*, 1003–1013; c) E. Iengo, E. Zangrando, E. Alessio, *Acc. Chem. Res.* **2006**, *39*, 841–851; d) E. Iengo, T. Gatti, E. Zangrando, M. T. Indelli, F. Scandola, E. Alessio, *Chem. Commun.* **2011**, *47*, 1616–1618; e) E. Alessio, M. Casanova, E. Zangrando, E. Iengo, *Chem. Commun.* **2012**, *48*, 5012–5015; f) E. Iengo, P. Cavigli, D. Milano, P. Tecilla, *Inorg. Chim. Acta* **2014**, *417*, 59–78.
[19] a) T. Gianferrara, I. Bratsos, E. Iengo, B. Milani, A. Oštrić, C. Spagnul, E. Zangrando, E. Alessio, *Dalton Trans.* **2009**, 10742–10756; b) T. Gianferrara, A. Bergamo, I. Bratsos, B. Milani, C. Spagnul, G. Sava, E. Alessio, *J. Med. Chem.* **2010**, *53*, 4678–4690.
[20] a) C. Spagnul, R. Alberto, G. Gasser, S. Ferrari, V. Pierroz, A. Bergamo, T. Gianferrara, E. Alessio, *J. Inorg. Biochem.* **2013**, *122*, 57–65; b) T. Gianferrara, C. Spagnul, R. Alberto, G. Gasser, S. Ferrari, V. Pierroz, A. Bergamo, E. Alessio, *ChemMedChem* **2014**, *9*, 1231–1237.
[21] E. Iengo, N. Demitri, G. Balducci, E. Alessio, *Dalton Trans.* **2014**, *43*, 12160–12163.
[22] F. Battistin, G. Balducci, N. Demitri, E. Iengo, B. Milani, E. Alessio, *Dalton Trans.* **2015**, *44*, 15671–15682.
[23] G. Mion, T. Gianferrara, A. Bergamo, G. Gasser, V. Pierroz, R. Rubbiani, R. Vilar, A. Leczkowska, E. Alessio, *ChemMedChem* **2015**, *10*, 1901–1914.
[24] E. Alessio, *Chem. Rev.* **2004**, *104*, 4203–4242.
[25] a) I. Bratsos, S. Jedner, A. Bergamo, G. Sava, T. Gianferrara, E. Zangrando, E. Alessio, *J. Inorg. Biochem.* **2008**, *102*, 1120–1133; b) G. Ragazzon, I. Bratsos, E. Alessio, L. Salassa, A. Habtemariam, R. McQuitty, G. J. Clarkson, P. J. Sadler, *Inorg. Chim. Acta* **2012**, *393*, 230–238; c) I. Finazzi, I. Bratsos, T. Gianferrara, A. Bergamo, N. Demitri, G. Balducci, E. Alessio, *Eur. J. Inorg. Chem.* **2013**, 4743–4753.
[26] C. A. Mebi, B. J. Frost, *Inorg. Chem.* **2007**, *46*, 7115–7120.
[27] R. Girotti, A. Romerosa, S. Mañas, M. Serrano-Ruiz, R. N. Perutz, *Inorg. Chem.* **2009**, *48*, 3692–3698.
[28] D. N. Akbayeva, S. Moneti, M. Peruzzini, L. Gonsalvi, A. Ienco, F. Vizza, *C. R. Chim.* **2005**, *8*, 1491–1496.
[29] F. Battistin, F. Scaletti, G. Balducci, S. Pillozzi, A. Arcangeli, L. Messori, E. Alessio, *J. Inorg. Biochem.* **2016**, DOI: 10.1016/j.jinorgbio.2016.02.009.
[30] In the ^{1}H NMR spectrum of **12** in $CDCl_3$, the most downfield signal, assigned to the NCH_2N protons of the equivalent PTA ligands, is a well-resolved AB quartet centered at δ = 4.50, rather than a singlet as reported in ref.[11]
[31] However, the ^{31}P chemical shift of coordinated PTA in D_2O depends on the pH and typically shifts to higher frequencies as the pH decreases. The largest shifts are encountered at pH values of ca. 3, which corresponds to the average pK_a of PTA coordinated to a Ru^{II} center. As an example, the titration of **16** is reported in the Supporting Information (Figure S40); see also ref.[11,13,14]
[32] In the *cis*-$RuH_2(PTA)_4$ complex, the ^{31}P NMR resonance of the two mutually *trans* PTAs falls way out of the expected range at δ = –26.6 ppm.
[33] S. Bolaño, J. Bravo, J. Castro, M. M. Rodriguez-Rocha, M. F. C. G. da Silva, A. J. L. Pombeiro, L. Gonsalvi, M. Peruzzini, *Eur. J. Inorg. Chem.* **2007**, 5523–5532.
[34] A. García-Fernández, J. Díez, A. Manteca, J. Sánchez, M. P. Gamasa, E. Lastra, *Polyhedron* **2008**, *27*, 1214–1228.
[35] S. Bolaño, M. M. Rodriguez-Rocha, J. Bravo, J. Castro, E. Onate, M. Peruzzini, *Organometallics* **2009**, *28*, 6020–6030.
[36] S. Miguel, J. Diez, M. P. Gamasa, M. E. Lastra, *Eur. J. Inorg. Chem.* **2011**, 4745–4755.
[37] A. García-Fernández, J. Díez, M. Pilar Gamasa, E. Lastra, *Eur. J. Inorg. Chem.* **2014**, 917–924.
[38] L. Leyva, C. Sirlin, L. Rubio, C. Franco, R. Le Lagadec, J. Spencer, P. Bischoff, C. Gaiddon, J.-P. Loeffler, M. Pfeffer, *Eur. J. Inorg. Chem.* **2007**, 3055–3066.
[39] I. Bratsos, E. Alessio, *Inorg. Synth.* **2010**, *35*, 148–152.
[40] I. Bratsos, C. Simonin, E. Zangrando, T. Gianferrara, A. Bergamo, E. Alessio, *Dalton Trans.* **2011**, *40*, 9533–9543.
[41] E. Iengo, E. Zangrando, E. Baiutti, F. Munini, E. Alessio, *Eur. J. Inorg. Chem.* **2005**, 1019–1031.
[42] D. G. McCafferty, B. M. Bishop, C. G. Wall, S. G. Hughes, S. L. Mecklenberg, T. J. Meyer, B. W. Erickson, *Tetrahedron* **1995**, *51*, 1093–1106.
[43] A. Lausi, M. Polentarutti, S. Onesti, J. R. Plaisier, E. Busetto, G. Bais, L. Barba, A. Cassetta, G. Campi, D. Lamba, A. Pifferi, S. C. Mande, D. D. Sarma, S. M. Sharma, G. Paolucci, *Eur. Phys. J. Plus* **2015**, *130*, 1–8.
[44] W. Kabsch, *Acta Crystallogr., Sect. D* **2010**, *66*, 125–132.
[45] M. C. Burla, R. Caliandro, B. Carrozzini, G. L. Cascarano, C. Cuocci, C. Giacovazzo, M. Mallamo, A. Mazzone, G. Polidori, *J. Appl. Crystallogr.* **2015**, *48*, 306–309.
[46] G. M. Sheldrick, *Acta Crystallogr., Sect. A* **2015**, *71*, 3–8.
[47] G. M. Sheldrick, *Acta Crystallogr., Sect. A* **2008**, *64*, 112–122.
[48] P. Emsley, K. Cowtan, *Acta Crystallogr., Sect. D* **2004**, *60*, 2126–2132.
[49] L. J. Farrugia, *J. Appl. Crystallogr.* **2012**, *45*, 849–854.

Received: January 30, 2016
Published Online: April 5, 2016